

Structural consequences of phosphorylation of two serine residues in the cytoplasmic domain of HIV-1 VpU

MARC WITTLICH, BERND W. KOENIG and DIETER WILLBOLD*

Institut für Neurowissenschaften und Biophysik, Biomolekulare NMR, Forschungszentrum Jülich, 52425 Jülich, Institut für Physikalische Biologie, Heinrich-Heine-Universität, BMFZ, 40225 Düsseldorf, Germany

Received 8 October 2007; Accepted 13 November 2007

Abstract: The human immunodeficiency virus type 1 (HIV-1) protein U (VpU) is an accessory protein responsible for enhancement of viral particle release and down regulation of the T-lymphocyte coreceptor CD4. Direct binding between the cytoplasmic domains of CD4 and VpU as well as phosphorylation of serines 53 and 57 in the cytoplasmic domain of VpU plays a central role in CD4 downregulation. We investigated structural consequences of phosphorylation of the two serines using nuclear magnetic resonance spectroscopy. A uniformly ^{15}N and ^{13}C stable isotope-labeled 45-residue peptide comprising the cytoplasmic domain of VpU (VpUcyt) was recombinantly produced in *E. coli*. The peptide forms two helices (commonly referred to as helix 2 and 3) in the presence of membrane mimicking dodecylphosphocholine (DPC) micelles, which flank a flexible region containing the two phosphorylation sites. Phosphorylation does not cause any drastic structural changes in the secondary structure of VpUcyt. However, an *N*-terminal elongation of helix 3 and a slightly reduced helicity at the *C*-terminus of helix 2 are observed upon phosphorylation based on characteristic changes of $^{13}\text{C}_\alpha$ and $^{13}\text{C}_\beta$ chemical shifts. Phosphorylation also reduces the local mobility of the protein backbone in the loop region containing the phosphorylation sites according to heteronuclear ^1H - ^{15}N nuclear Overhauser enhancement (NOE) data. Copyright © 2008 European Peptide Society and John Wiley & Sons, Ltd.

Keywords: HIV-1; VpU; CD4; phosphorylation; NMR; viral accessory protein

INTRODUCTION

The 81-residue transmembrane protein VpU is one of the accessory proteins encoded in the genome of the HIV-1 [1–4]. A short stretch of basic amino acids separates the *N*-terminal transmembrane part of VpU (α -helix 1 [5]) from the acidic cytoplasmic domain. There is consensus on formation of an α -helix 2 – flexible loop – α -helix 3 motif in the cytoplasmic region of VpU followed either by a *C*-terminal turn [6] or by a short fourth helix [7] in membrane-like environments (recently reviewed in [8]). The flexible loop comprises two serine residues (Ser53 and Ser57 in VpU of HIV strain HV1S1) that are part of a highly conserved dodecapeptide sequence extending from Glu48 to Gly59 [7] and are subject to phosphorylation by CK2 [9].

Two major functions of VpU have been reported. The ability of VpU to enhance progeny virus release has been attributed to the transmembrane region, whereas the CD4 downregulation activity was traced to the cytoplasmic domain [10]. VpU binds directly to newly

synthesized CD4 that is trapped in a complex with viral envelope precursor protein gp160 in the endoplasmic reticulum and induces rapid degradation of the viral receptor CD4 in the cytosolic ubiquitin–proteasome pathway [11]. The membrane proximal amphipathic helix 2 and *C*-terminal residues of the cytoplasmic domain of VpU are important for CD4 binding [12]. Phosphorylation of Ser53 and Ser57 of VpU by CK2 is not required for binding CD4, but is essential for CD4 degradation [13,14]. Phosphorylated VpU binds human β TrCP, which in turn binds the proteasome-targeting factor Skp1p, resulting in a multiprotein complex that connects CD4 to degradation by the proteasome pathway [15].

Secondary structure elements of the cytoplasmic domain of VpU have been derived from solution NMR data on various VpU polypeptide fragments recorded in TFE–water mixtures [6,16], high salt aqueous solution [7], and DHPC micellar solution [17]. Although the helix 2 – loop – helix 3 motif is generally accepted, the exact location and extension of these elements differ somewhat depending on experimental conditions (buffer solution, fragment length, temperature, pH, etc.).

Despite the functional significance of VpU phosphorylation, there is very little data on its effect on VpU structure. The orientation of helix 2 parallel to the lipid membrane surface is not affected by phosphorylation of VpU according to solid state NMR on the VpU(27–57) polypeptide [18]. Coadou *et al.* used solution NMR to study the truncated peptide VpU(41–61) in water and

Abbreviations: HIV-1, human immunodeficiency virus type 1; VpU, virus protein U; NMR, nuclear magnetic resonance; HSQC, heteronuclear single quantum coherence; NOE, nuclear Overhauser enhancement; NOESY, NOE spectroscopy; TROSY, transverse relaxation optimized spectroscopy; CK2, casein kinase II; DPC, dodecylphosphocholine; GSH, glutathione sepharose; IPTG, isopropyl- β -D-1-thiogalactopyranoside; RPC, reversed phase chromatography.

*Correspondence to: Dieter Willbold, INB-2, Forschungszentrum Jülich, D-52425 Jülich, Germany;
e-mail: dieter.willbold@uni-duesseldorf.de

in TFE solution both in the presence and absence of serine phosphorylation [19]. The peptide used in their study contained the flexible loop region and parts of the flanking cytoplasmic helices 2 and 3. Following phosphorylation, the α -helix 3 fragment was no longer observed. Instead, a short β -strand emerged close to the C-terminus of the peptide. A very similar structure of phosphorylated VpU(41–61) was reported for the β TrCP-bound peptide [20]. In contrast, a recent molecular dynamics simulation on full length VpU in a lipid bilayer indicated that phosphorylation of VpU reduces the helicity of several residues at the termini of both helices 2 and 3 adjacent to the loop region but no β -strand formation was reported [21].

Post-translational phosphorylation is a highly abundant mechanism for regulation of protein activity. Occasionally, side chain phosphorylation causes global structural changes of the affected protein [22]. More frequently, phosphorylation results in minor conformational changes only [23]. In particular, phosphorylation can stabilize the N-terminus of a proximate α -helix [24]. The objective of our study was the investigation of the structural consequences of phosphorylation of Ser53 and Ser57 of VpU by CK2. VpU is a trans-membrane protein and its cytoplasmic domain resides in the polar lipid–water interface region of the membrane. Therefore, it is crucial that the structure of the cytoplasmic domain of VpU is studied in an appropriate environment. However, high resolution liquid state NMR spectroscopy is only feasible with model membrane particles of limited size which must undergo rather rapid rotational diffusion. We investigated the behavior of the cytoplasmic domain of the HIV-1 protein VpU as a function of phosphorylation in the presence of membrane-mimicking DPC micelles.

MATERIALS AND METHODS

Protein Expression and Purification

A DNA fragment coding for the cytoplasmic domain of VpU (residues 39–81; residue numbering scheme of the HIV-1 strain HV1S1, Swiss-Prot accession number P19554) was amplified by PCR and cloned into the vector pGEX-2T (GE Healthcare) using BamHI and NotI restriction sites. The new vector pGEX-2T-VpUcyt was used for transformation of *E. coli* BL21(DE3) cells (Invitrogen). Cells were grown at 37 °C until the absorbance at 600 nm had reached the value of ~ 0.7 . Expression of the fusion protein was induced by addition of IPTG to a final concentration of 1 mM. The cells were harvested following another 4 h of shaking at 37 °C after induction. For ^{15}N and/or ^{13}C isotopic labeling, M9 minimal medium [25] was employed with ^{15}N ammonium chloride and ^{13}C glucose (Cambridge Isotope Laboratories) as the sole nitrogen and carbon sources, respectively. The Gly-Ser-Thr–VpUcyt fusion protein was purified using affinity chromatography on GSH 4B (GE Healthcare). The fusion protein contains a thrombin cleavage site that immediately

precedes the VpU(39–81) sequence. Enzymatic cleavage with thrombin protease (GE Healthcare) was performed on a GSH column resulting in release of the 45-residue target protein consisting of VpU(39–81) with an additional N-terminal Gly–Ser dipeptide. This 45-residue polypeptide is referred to as VpUcyt in what follows. VpUcyt was further purified by RPC using a Resource 15 RPC 3 ml column (GE Healthcare) equilibrated with 50 mM ammonium acetate at pH 7.2. The protein was eluted from the column using a water–acetonitrile gradient. VpUcyt containing fractions were pooled, lyophilized, and stored at -20°C until use.

Phosphorylation Reaction and Dephosphorylation Assay

CK2 was purchased from New England Biolabs. Lyophilized VpUcyt was dissolved at a concentration of 1 mM in 0.5 ml phosphate buffer [20 mM sodium phosphate, pH 7.5, 100 mM NaCl, 10 mM MgCl_2 , 400 μM ATP, 100 mM DPC-d38 in $\text{H}_2\text{O}/^2\text{H}_2\text{O}$ (9:1, v/v)]. DPC-d38 and $^2\text{H}_2\text{O}$ were from Cambridge Isotope Laboratories. 3000 units of CK2 were added and the phosphorylation reaction was allowed to proceed for 1 h at 30 °C resulting in virtually quantitative phosphorylation of Ser53 and Ser57. The degree of phosphorylation was checked by recording a ^1H , ^{15}N -HSQC NMR spectrum of VpUcyt after adjusting the sample pH to 6.2. Phosphorylation causes distinct changes of the backbone amide ^1H N and ^{15}N chemical shifts of the affected residues [26] (Figure 1). Only one set of VpUcyt resonances was observed in the HSQC spectrum after 1 h of incubation with CK2, indicating that the phosphorylation reaction was complete. Phosphorylated VpUcyt was purified from CK2 and nucleotides by RP-HPLC following the protocol described above.

The effect of CK2 on VpUcyt was fully reversible by enzymatic dephosphorylation, confirming that the employed CK2

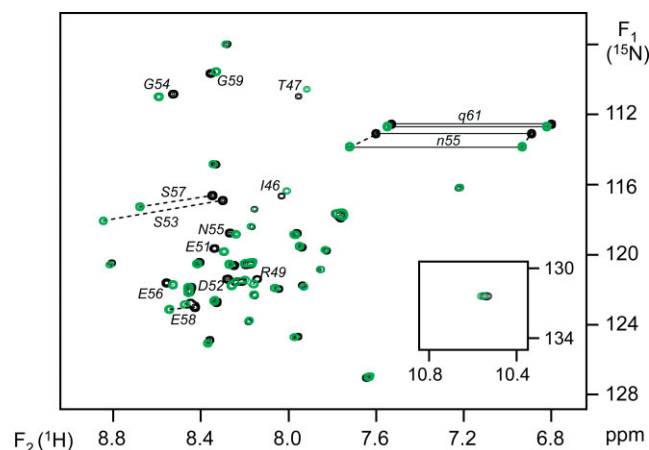


Figure 1 ^1H , ^{15}N -HSQC spectra of ^{15}N -labeled VpUcyt with phosphorylated (green) and unphosphorylated (black) Ser53 and Ser57 recorded in 100 mM DPC-d38 at 30 °C and pH 6.2. Phosphorylation induces strong chemical shifts changes of the amide protons and nitrogens of Ser53 and Ser57. Additional residues that undergo moderate but significant resonance shifts are annotated. Backbone and side chain amides are denoted by capital and lower case letters, respectively. The insert shows the indole ring HN–N correlation of Trp76.

did not contain or cause any activities other than phosphorylation of VpUcyt (e.g. proteolytic activity). Incubation of 125 μM phosphorylated ^{15}N -labeled VpUcyt in 0.3 ml reaction buffer with 10 units of shrimp alkaline phosphatase (SAP; purchased from MBI Fermentas) for 1.5 h at 37 °C resulted in complete reversion of the HSQC spectrum into that of nonphosphorylated VpUcyt.

The identity of both nonphosphorylated and phosphorylated VpUcyt proteins was confirmed based on molecular mass determination by electrospray ionization mass spectrometry.

NMR Spectroscopy

NMR samples contained 1 mM VpUcyt and 100 mM DPC-d38 in phosphate buffer [20 mM sodium phosphate, pH 6.2, 100 mM NaCl, 0.02% (w/v) NaN_3 in $\text{H}_2\text{O}/^2\text{H}_2\text{O}$ (9:1, v/v)]. Samples were prepared using either phosphorylated or unphosphorylated VpUcyt, respectively.

NMR spectra were acquired at 30 °C on Varian Unity INOVA spectrometers operating at ^1H resonance frequencies of 600 and 800 MHz, respectively. Triple resonance $^1\text{H}\{^{13}\text{C},^{15}\text{N}\}$ probes equipped with actively shielded three-axis pulsed field gradient (PFG) or z-axis PFG coils were employed for measurements at 14.1 and 18.8 T, respectively. Data were processed with NMR Pipe [27] or VNMRJ (Varian, Inc.), and analyzed with CARA [28].

Sequential assignment of ^1HN , ^{15}N , $^{13}\text{C}_\alpha$, and $^{13}\text{C}_\beta$ resonances of VpUcyt was accomplished based on $^1\text{H},^{15}\text{N}$ -HSQC [29], gradient enhanced $^1\text{H},^{13}\text{C}$ -HSQC [30], and HNCACB [31] experiments at 14.1 T. All resonances were referenced to internal 2,2-dimethyl-2-silapentane-5-sulfonic acid (DSS).

Heteronuclear $^1\text{H}-^{15}\text{N}$ NOEs were derived from two-dimensional spectra recorded at 18.8 T with a TROSY [32] based NOE pulse sequence [33]. $^1\text{H}-^{15}\text{N}$ NOE-TROSY spectra were acquired with or without 3 s of ^1H saturation prior to the first pulse of the NOE sequence. A series of 120° pulses spaced at 5 ms intervals was used for proton saturation. NOE intensities were obtained by fitting NOE peaks to an adjustable 'model peak' shape using CARA. A superposition of Gauss and Lorentz functions was employed. The model parameters (Gauss-Lorentz balance, line width) were adjusted manually and independently for both spectral dimensions using representative NOE peaks. The complete list of NOE intensities was obtained by fitting all NOE peaks of a given spectrum against the same 'model peak' shape. The heteronuclear NOE is the ratio of the integral peak intensities measured with and without proton presaturation, respectively.

RESULTS AND DISCUSSION

Mapping of Chemical Shift Changes upon Phosphorylation

The resonance frequency of a nuclear spin reflects the effective magnetic flux density at the position of the nucleus and depends on both the field of the NMR magnet and the electronic environment of the nucleus. The exact position of an NMR signal is affected by chemical modifications if they influence the local electron density, e.g. due to inductive or mesomeric substituent

effects transmitted through chemical bonds. Through space interactions with magnetically anisotropic moieties are another source of resonance shifts. Chemical shifts of nuclei in the backbone of a protein are influenced to various extents by geometry, hydrogen bonding, and the attached side chain [34]. Characteristic deviations of chemical shifts from values typically observed in unstructured proteins (referred to as random coil shifts) provide a sensitive indicator of secondary structure [35]. However, chemical modification of an amino acid residue may also cause substantial chemical shift changes of nearby nuclei independently of the secondary structure context. For example, phosphorylation of serine residues in unstructured peptides causes chemical shift changes of serine resonances that depend on the ionization state of the phosphate group and can be comparable in magnitude to changes resulting from secondary structure formation [26].

Figure 1 shows a superposition of $^1\text{H},^{15}\text{N}$ -HSQC spectra of phosphorylated (green) and unphosphorylated (black) VpUcyt in DPC micelle solution. All expected backbone and side chain amide correlations have been identified, but only peaks undergoing a significant shift upon phosphorylation are labeled in the figure. Large shifts are observed for Ser53 and Ser57. In addition, small but significant shifts occur for almost all backbone amides in the sequence from Ile46 to Gly59 and for the side chain amides of Asn55 and Gln61.

Phosphorylation of serine residues in unstructured peptides has been reported to induce chemical shift changes of $\Delta\delta^{\text{HN}} \sim 0.3$ ppm and $\Delta\delta^{\text{N}} \sim -0.2$ ppm (monoanionic phosphate group) or $\Delta\delta^{\text{HN}} \sim 1$ ppm and $\Delta\delta^{\text{N}} \sim 2.8$ ppm (dianionic phosphate group) [26] relative to unphosphorylated peptides [34]. The observed shifts of Ser53 ($\Delta\delta^{\text{HN}} \sim 0.5$ ppm; $\Delta\delta^{\text{N}} \sim 1.2$ ppm) and Ser57 ($\Delta\delta^{\text{HN}} \sim 0.3$ ppm; $\Delta\delta^{\text{N}} \sim 0.6$ ppm) are between these values. The pKa of the equilibrium of mono- and dianionic forms of phosphorylated serine is about 6 [26]. At pH 6.2, where the present NMR study was conducted, a mixture of both ionic forms with rapid fluctuations of the charge state of individual phosphate groups is expected, resulting in intermediate chemical shifts in agreement with our data. The substantial $\Delta\delta^{\text{HN}}$ and $\Delta\delta^{\text{N}}$ shifts of Ser53 and Ser57 of VpUcyt observed upon phosphorylation are, at least to a large part, a direct effect of the modified electron density at the position of the observed spins induced by the substituent. The minor chemical shift changes throughout the sequence from Ile46 to Gly59 (Figure 2) may reflect slight modifications of the structure or dynamic properties of the affected region due to steric and/or electrostatic effects of the covalently attached charged phosphate moieties.

Secondary Structure Estimation using Carbon Chemical Shift Data

The influence of serine phosphorylation on secondary structure of VpUcyt is examined in Figure 3 based on

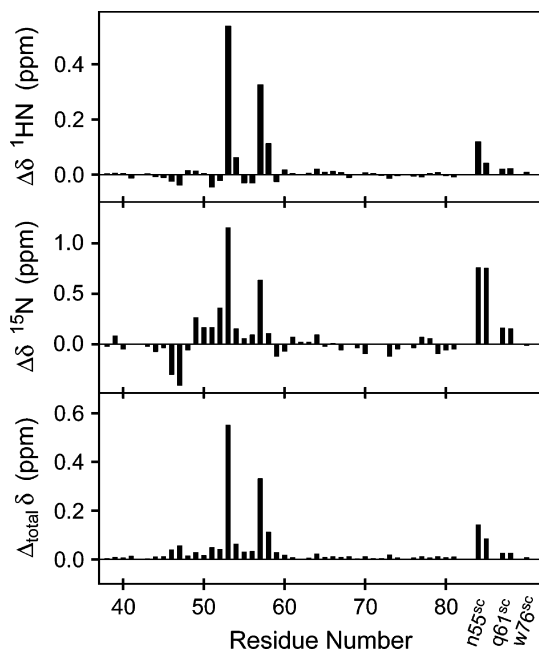


Figure 2 Histograms of chemical shift changes of VpUcyt backbone and side chain $^1\text{H-N}$ (above) and ^{15}N (middle) resonances resulting from phosphorylation of Ser53 and Ser57. The lower panel shows total chemical shift changes according to the equation $\Delta_{\text{total}}\delta = [(\Delta\delta\text{H})^2 + (0.1 \times \Delta\delta\text{N})^2]^{1/2}$ [36].

$\Delta\delta^{13\text{C}} = \Delta\delta^{13\text{C}_\alpha} - \Delta\delta^{13\text{C}_\beta}$ values, which combine the sensitivity of protein $^{13\text{C}_\alpha}$ and $^{13\text{C}_\beta}$ chemical shifts for protein secondary structure elements. In general, $^{13\text{C}_\alpha}$ resonances experience an average downfield shift of ~ 2.5 ppm in helices and an average upfield shift of ~ 2.0 ppm in β -sheets relative to random coil shifts, while $^{13\text{C}_\beta}$ shifts show little deviation from random coil values in helices, but are shifted downfield by ~ 2.5 ppm in β -sheets [34]. The chemical shift changes $\Delta\delta^{13\text{C}_\alpha}$ and $\Delta\delta^{13\text{C}_\beta}$ represent the difference between the measured $^{13\text{C}_\alpha}$ and $^{13\text{C}_\beta}$ chemical shifts and tabulated, amino acid-specific random coil shift values, respectively [37]. In a $\Delta\delta^{13\text{C}}$ plot (upper two panels of Figure 3), a dense grouping of four or more positive bars, each exceeding a threshold of 0.7 ppm, with an average height of ~ 2.5 ppm indicates helical structure. A cluster of three or more negative bars, each smaller than -1.4 ppm, with an average magnitude ~ 4.5 ppm strongly hints at a β -strand conformation [34,35].

Figure 3 clearly indicates the presence of two helices in VpUcyt both in the absence (top panel) and presence (middle panel) of serine phosphorylation in DPC micelles. Most likely, helix 2 extends from the *N*-terminal Ile39 of the VpUcyt sequence through Glu48 and helix 3 from Leu64 through Arg70 (we follow the generally accepted VpU helix numbering scheme introduced above). The extent of the two helices is indicated by a gray background in Figure 3. The average magnitude of $\Delta\delta^{13\text{C}}$ in helix 2 is significantly larger

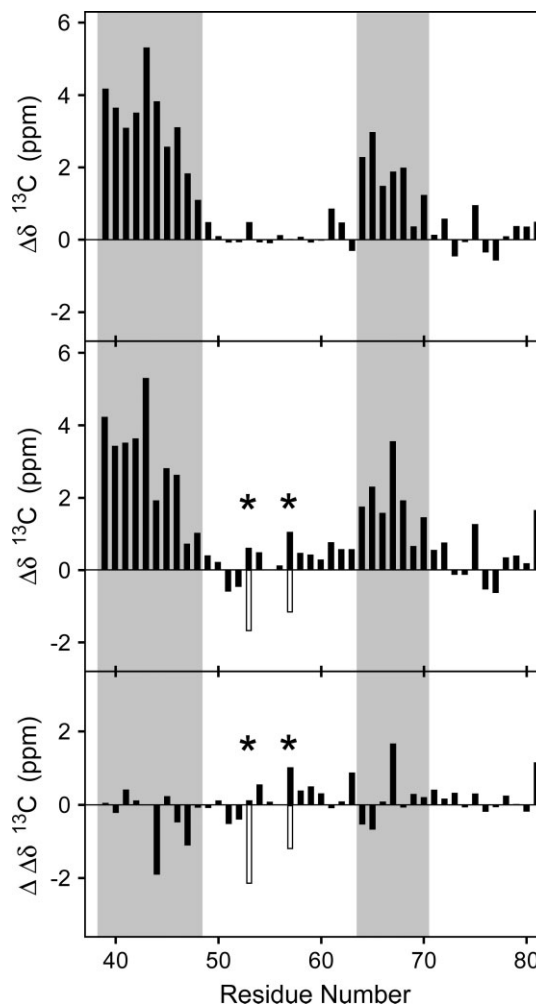


Figure 3 Effect of phosphorylation of Ser53 and Ser57 on secondary chemical shifts of VpUcyt studied in detergent micelles (100 mM DPC-d38) at 30°C . The upper two panels show the difference $\Delta\delta^{13\text{C}_\alpha} - \Delta\delta^{13\text{C}_\beta}$ in case of unphosphorylated (top) and phosphorylated (middle) VpUcyt. $\Delta\delta$ denotes the difference between observed and tabulated random coil chemical shifts [37]. The lower panel displays the difference between the $\Delta\delta$ values in the upper two panels (phosphorylated–unphosphorylated state). The position of the two phosphorylated serines is indicated by asterisks. Random coil chemical shifts of Ser53 and Ser57 were corrected for the direct shift caused by phosphorylation assuming either a monoanionic (solid bars) or a dianionic phosphate group (open bars) [26]. Two regions with pronounced helix propensity are observed in VpUcyt (amino acids 39–48 and 64–70, highlighted by gray background) and appear to be rather insensitive to the phosphorylation state.

than in helix 3, indicating a higher degree of helicity in the *N*-terminal helix. Most likely, helix 2 is adopted in almost all VpUcyt molecules in the NMR sample while helix 3 is present in less than 40% of the polypeptides at any instant of time due to substantial conformational exchange in this part of the peptide.

The region between the two helices shows no apparent preference for helical or β -strand conformations

in the unphosphorylated VpUcyt. Phosphorylation of Ser53 and Ser57 causes large chemical shift changes of the $^{13}\text{C}_\beta$ and moderate changes of the $^{13}\text{C}_\alpha$ serine resonance positions. However, taking into account the influence of serine phosphorylation on random coil shifts of serine [26] reduces the $\Delta\delta^{13}\text{C}$ values of Ser53 and Ser57 (marked by asterisks in Figure 3, middle) to low levels. Filled and open bars represent $\Delta\delta^{13}\text{C}$ values calculated with random coil shifts of serine bound to either mono- or dianionic phosphate, respectively. Rapid exchange between the mono- and dianionic charge state of the phosphate group, as expected at the pH 6.2 of this study (see above), will result in effective $\Delta\delta^{13}\text{C}$ values of Ser53 and Ser57 intermediate between the open and closed bars, i.e. even closer to zero. All other residues in the region between helices 2 and 3 show $\Delta\delta^{13}\text{C}$ values at (Gln61) or below the threshold of 0.7 ppm for helix formation. Clearly, there is also no indication for β -strand formation in this region. If anything, the uninterrupted stretch of small positive $\Delta\delta^{13}\text{C}$ values between Ser57 and Leu64 observed in Figure 3 (middle) might hint at an *N*-terminal extension of helix 3 in a subfraction of phosphorylated VpUcyt conformers.

The lower panel of Figure 3 shows the difference between $\Delta\delta^{13}\text{C}$ in phosphorylated versus unphosphorylated VpUcyt. The aim of this graph is to highlight changes in helix or β -strand propensity that might occur as a result of phosphorylation. No pronounced changes on the secondary structure level are visible. Nevertheless, there might be minor modifications of the conformational ensemble of VpUcyt. Clustering of three negative bars in the *C*-terminal half of helix 2 is compatible with a slightly reduced helicity of the last turn of this helix, i.e. helix 2 might be shortened in a fraction of the phosphorylated VpUcyt conformers. The possible *N*-terminal extension of helix 3 mentioned above is also reflected by a series of positive bars between Ser57 and Leu64 in the lower panel.

In a regular α -helix, the dipole moments of the individual peptide units are aligned almost parallel to the helix axis resulting in a substantial net dipole moment referred to as helix dipole [38]. The positive end of the helix dipole points towards the *N*-terminus and the negative dipole end towards the *C*-terminus of the α -helix. Introduction of a negative charge in the vicinity of the *N*-terminus of an α -helix is expected to stabilize the helix but placing the negative charge close to the *C*-terminus should have a helix destabilizing effect [39]. Phosphorylation of Ser53 and Ser57 introduces negative charges to the flexible loop region connecting helices 2 and 3 of VpUcyt (Figure 4). It is conceivable that electrostatic interactions of the negatively charged phosphate with the positive end of the dipole of helix 3 causes an *N*-terminal stabilization of helix 3 while unfavorable interactions with the negative end of the dipole of helix 2 destabilize the *C*-terminus of helix 2. Alternatively, extension of helix 3 in some of the

dynamically exchanging conformers may be explained by direct hydrogen bond formation between one of the four unsatisfied backbone amide hydrogen donors at the *N*-terminus of the elongated helix and a negatively charged or polar side chain in the *N*-cap position of the helix without the need to invoke a helix macrodipole [24]. Indeed, Ser57 appears to occupy the *N*-cap position in the conformers with an elongated helix 3 in phosphorylated VpUcyt as indicated by the stretch of positive $\Delta\delta^{13}\text{C}$ values between Ser57 and Leu64 which marks the *N*-terminus of helix 3 in unphosphorylated VpUcyt (Figure 4, middle panel).

Dynamic Characterization of VpUcyt by ^1H - ^{15}N -hetero-NOE Data

The heteronuclear $\{^1\text{H}\}$ - ^{15}N NOE is a sensitive indicator of local variations in protein backbone motions on the pico- to nanosecond time scale. The overall isotropic tumbling motion of a DPC micelle associated VpUcyt protein should have a rotational correlation time of the order of 9 ns [40]. If the complex tumbles as a rigid unit lacking fast internal motions of protein backbone *N*-H bond vectors, one should observe positive ^1H - ^{15}N NOEs close to the value of ~ 0.8 representing the slow motion limit [41]. Rapid internal motion will reduce the size of the NOE that may become negative for highly mobile residues exhibiting large amplitude motions on a subnanosecond time scale [42].

We employed ^1H - ^{15}N -hetero-NOE data [41] to analyze the local mobility of VpUcyt in a residue specific manner. Figure 5 shows ^1H - ^{15}N NOEs of VpUcyt backbone amides in the presence of DPC micelles both with and without protein phosphorylation. In either case, two regions with relatively large heteronuclear NOEs are observed indicating reduced dynamics. These regions include the location of helices 2 and 3 of VpUcyt. Residues at the *C*-terminus of VpUcyt are highly flexible, while the backbone amides in the loop region connecting the two helices exhibit intermediate mobility. Interestingly, phosphorylation of Ser53 and Ser57 causes a localized reduction in mobility that is restricted to this interconnecting loop region. Introduction of two bulky and charged phosphate groups apparently restricts the ensemble of conformations that are sampled by the loop, perhaps due to electrostatic interactions and/or steric

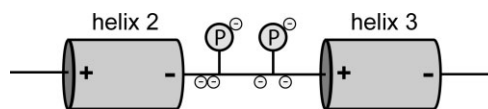


Figure 4 Sketch of the secondary structure elements of VpUcyt. Negative charges in the loop connecting the helices are denoted by an encircled minus sign, the introduced phosphate groups by an encircled P. Although monoanionic phosphate groups are depicted, rapid interconversion between mono- and dianionic forms of both phosphate moieties is very likely.

hindrance. The localized change in mobility of residues 53 through 59 is clearly demonstrated by the difference plot of the NOE values measured with and without phosphorylation of VpUcyt, respectively (Figure 5, lower panel). The phosphorylation-induced *N*-terminal stabilization and/or extension of helix 3 discussed above could be partially responsible for the reduced mobility of the loop residues.

Altogether, phosphorylation of Ser53 and Ser57 does not cause pronounced structural changes of the cytoplasmic domain of VpU in the presence of membrane-like DPC micelles. This observation is in contrast to a previous solution NMR study on structural effects of phosphorylation in the shorter peptide VpU(41–61) in water and in TFE solution by Coadou and coworkers [19]. Their peptide contained the flexible

loop region and parts of the flanking cytoplasmic helices 2 and 3. Only the unphosphorylated VpU(41–61) but not the phosphorylated peptide exhibited helical features at the *C*-terminus reminiscent of a fragment of α -helix 3. Instead, a short β -strand was observed close to the *C*-terminus of the phosphorylated peptide. The authors proposed a conformational switch mechanism for functional activation of VpU that is triggered by dual serine phosphorylation [19].

Based on our study of the complete cytoplasmic domain of VpU in the presence of membrane-mimicking micelles, we can clearly rule out drastic phosphorylation-induced conformational changes such as β -strand formation. Most likely, the small size of the VpU(41–61) peptide and/or the solvent conditions used in the study of Coadou and colleagues are responsible for the apparent discrepancy with our observations.

Interestingly, a recent molecular dynamics simulation on full length VpU in a lipid bilayer predicted that phosphorylation of VpU reduces the helicity of several residues at the termini of both helices 2 and 3 proximal to the loop region [21]. Although our data support a slightly reduced helicity at the *C*-terminus of helix 2 after phosphorylation (*cf* the pronounced negative $\Delta\delta^{13}\text{C}$ values of residues 44 and 47 in the lower panel of Figure 3), the experimentally observed *N*-terminal extension of helix 3 is not in full agreement to the prediction.

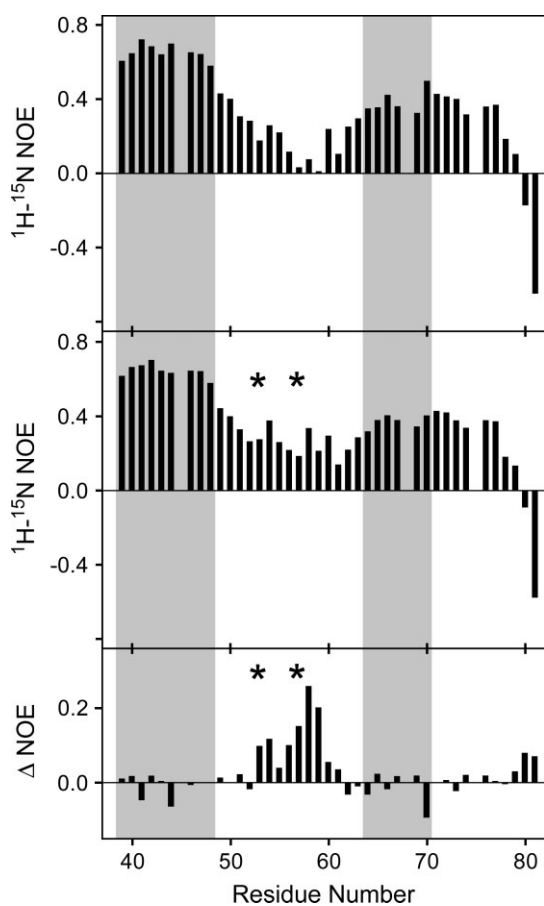


Figure 5 Effect of phosphorylation of Ser53 and Ser57 on the backbone dynamics of VpUcyt studied in detergent micelles (100 mM DPC-d38) at 30 °C. Shown are steady-state heteronuclear ^1H - ^{15}N NOE data of unphosphorylated (top) and phosphorylated (middle) VpUcyt. The lower panel displays the difference between the two NOE data sets (phosphorylated – unphosphorylated state). Asterisks mark the position of the phosphorylated Ser53 and Ser57. The most likely extension of helices 2 and 3 as derived from chemical shift analysis is indicated by a gray background. No data could be obtained for Arg45 and Val68 due to strong peak overlap and for residue 75, which is a proline.

CONCLUSIONS

Phosphorylation of Ser53 and Ser57 of VpU has only a very modest influence on the structure of the cytoplasmic domain of the HIV-1 protein in a membrane-like environment. Phosphorylation causes a slight *N*-terminal stabilization and elongation of helix 3 that is accompanied by reduced mobility of residues in the flexible loop connecting helices 2 and 3, and perhaps a reduction of helicity at the *C*-terminal end of helix 2. Phosphorylation of VpU does not cause drastic structural changes but rather introduces epitope details that are essential for recognition of Vpu by downstream effectors, like βTrCP .

Acknowledgements

This work was supported by a grant from the 'Präsidentenfond der Helmholtzgemeinschaft' (HGF, 'Virtual Institute of Structural Biology') to D.W.

REFERENCES

1. Strebel K, Klimkait T, Martin MA. A novel gene of HIV-1, vpu, and its 16-kilodalton product. *Science* 1988; **241**: 1221–1223.
2. Cohen EA, Terwilliger EF, Sodroski JG, Haseltine WA. Identification of a protein encoded by the vpu gene of HIV-1. *Nature* 1988; **334**: 532–534.

3. Trono D. HIV accessory proteins: leading roles for the supporting cast. *Cell* 1995; **82**: 189–192.
4. Strebel K. HIV accessory genes Vif and Vpu. *Adv. Pharmacol.* 2007; **55**: 199–232.
5. Marassi FM, Ma C, Gratkowski H, Straus SK, Strebel K, Oblatt-Montal M, Montal M, Opella SJ. Correlation of the structural and functional domains in the membrane protein Vpu from HIV-1. *Proc. Natl. Acad. Sci. U.S.A.* 1999; **96**: 14336–14341.
6. Wray V, Federau T, Henklein P, Klabunde S, Kunert O, Schomburg D, Schubert U. Solution structure of the hydrophilic region of HIV-1 encoded virus protein U (Vpu) by CD and ¹H NMR spectroscopy. *Int. J. Pept. Protein Res.* 1995; **45**: 35–43.
7. Willbold D, Hoffmann S, Rosch P. Secondary structure and tertiary fold of the human immunodeficiency virus protein U (Vpu) cytoplasmic domain in solution. *Eur. J. Biochem.* 1997; **245**: 581–588.
8. Wray V, Schubert U. Structure, phosphorylation, and biological function of the HIV-1 specific virus protein U (Vpu). In *Viral Membrane Proteins: Structure, Function, Drug Design*, Fischer WB (ed.). Kluwer Academic/Plenum Publishers: New York, 2005; 165–175.
9. Schubert U, Schneider T, Henklein P, Hoffmann K, Berthold E, Hauser H, Pauli G, Porstmann T. Human-immunodeficiency-virus-type-1-encoded Vpu protein is phosphorylated by casein kinase II. *Eur. J. Biochem.* 1992; **204**: 875–883.
10. Schubert U, Bour S, Ferrer-Montiel AV, Montal M, Maldarelli F, Strebel K. The two biological activities of human immunodeficiency virus type 1 Vpu protein involve two separable structural domains. *J. Virol.* 1996; **70**: 809–819.
11. Willey RL, Maldarelli F, Martin MA, Strebel K. Human immunodeficiency virus type 1 Vpu protein induces rapid degradation of CD4. *J. Virol.* 1992; **66**: 7193–7200.
12. Margottin F, Benichou S, Durand H, Richard V, Liu LX, Gomas E, Benarous R. Interaction between the cytoplasmic domains of HIV-1 Vpu and CD4: role of Vpu residues involved in CD4 interaction and in vitro CD4 degradation. *Virology* 1996; **223**: 381–386.
13. Schubert U, Strebel K. Differential activities of the human immunodeficiency virus type 1-encoded Vpu protein are regulated by phosphorylation and occur in different cellular compartments. *J. Virol.* 1994; **68**: 2260–2271.
14. Bour S, Schubert U, Strebel K. The human immunodeficiency virus type 1 Vpu protein specifically binds to the cytoplasmic domain of CD4: implications for the mechanism of degradation. *J. Virol.* 1995; **69**: 1510–1520.
15. Margottin F, Bour SP, Durand H, Selig L, Benichou S, Richard V, Thomas D, Strebel K, Benarous R. A novel human WD protein, h-beta TrCp, that interacts with HIV-1 Vpu connects CD4 to the ER degradation pathway through an F-box motif. *Mol. Cell.* 1998; **1**: 565–574.
16. Federau T, Schubert U, Flossdorf J, Henklein P, Schomburg D, Wray V. Solution structure of the cytoplasmic domain of the human immunodeficiency virus type 1 encoded virus protein U (Vpu). *Int. J. Pept. Protein Res.* 1996; **47**: 297–310.
17. Ma C, Marassi FM, Jones DH, Straus SK, Bour S, Strebel K, Schubert U, Oblatt-Montal M, Montal M, Opella SJ. Expression, purification, and activities of full-length and truncated versions of the integral membrane protein Vpu from HIV-1. *Protein Sci.* 2002; **11**: 546–557.
18. Henklein P, Kinder R, Schubert U, Bechinger B. Membrane interactions and alignment of structures within the HIV-1 Vpu cytoplasmic domain: effect of phosphorylation of serines 52 and 56. *FEBS Lett.* 2000; **482**: 220–224.
19. Coadou G, Evrard-Todeschi N, Gharbi-Benarous J, Benarous R, Girault JP. HIV-1 encoded virus protein U (Vpu) solution structure of the 41–62 hydrophilic region containing the phosphorylated sites Ser52 and Ser56. *Int. J. Biol. Macromol.* 2002; **30**: 23–40.
20. Coadou G, Gharbi-Benarous J, Megy S, Bertho G, Evrard-Todeschi N, Segéral E, Benarous R, Girault JP. NMR studies of the phosphorylation motif of the HIV-1 protein Vpu bound to the F-box protein beta-TrCP. *Biochemistry* 2003; **42**: 14741–14751.
21. Lemaitre V, Willbold D, Watts A, Fischer WB. Full length Vpu from HIV-1: combining molecular dynamics simulations with NMR spectroscopy. *J. Biomol. Struct. Dyn.* 2006; **23**: 485–496.
22. Johnson LN, Lewis RJ. Structural basis for control by phosphorylation. *Chem. Rev.* 2001; **101**: 2209–2242.
23. Groban ES, Narayanan A, Jacobson MP. Conformational changes in protein loops and helices induced by post-translational phosphorylation. *PLoS Comput. Biol.* 2006; **2**: e32.
24. Smart JL, McCammon JA. Phosphorylation stabilizes the N-termini of alpha-helices. *Biopolymers* 1999; **49**: 225–233.
25. Sambrook J, Russell DW. *Molecular Cloning: A Laboratory Manual*. Cold Spring Harbor Laboratory Press: Cold Spring Harbor, 2001.
26. Bienkiewicz EA, Lumb KJ. Random-coil chemical shifts of phosphorylated amino acids. *J. Biomol. NMR* 1999; **15**: 203–206.
27. Delaglio F, Grzesiek S, Vuister GW, Zhu G, Pfeifer J, Bax A. NMRPipe: a multidimensional spectral processing system based on UNIX pipes. *J. Biomol. NMR* 1995; **6**: 277–293.
28. Keller RLJ. *The Computer Aided Resonance Assignment Tutorial*. CANTINA Verlag: Goldau, 2004.
29. Bodenhausen G, Ruben DJ. Natural abundance nitrogen-15 NMR by enhanced heteronuclear spectroscopy. *Chem. Phys. Lett.* 1980; **69**: 185–189.
30. Kay LE, Keifer P, Saarinen T. Pure absorption gradient enhanced heteronuclear single quantum correlation spectroscopy with improved sensitivity. *J. Am. Chem. Soc.* 1992; **114**: 10663–10665.
31. Wittekind M, Mueller L. HNCACB, a high-sensitivity 3D NMR experiment to correlate amide-proton and nitrogen resonances with the alpha- and beta-carbon resonances in proteins. *J. Magn. Reson. B* 1993; **101**: 201–205.
32. Pervushin K, Riek R, Wider G, Wuthrich K. Attenuated T2 relaxation by mutual cancellation of dipole-dipole coupling and chemical shift anisotropy indicates an avenue to NMR structures of very large biological macromolecules in solution. *Proc. Natl. Acad. Sci. U.S.A.* 1997; **94**: 12366–12371.
33. Zhu G, Xia Y, Nicholson LK, Sze KH. Protein dynamics measurements by TROSY-based NMR experiments. *J. Magn. Reson.* 2000; **143**: 423–426.
34. Wishart DS, Case DA. Use of chemical shifts in macromolecular structure determination. *Meth. Enzymol.* 2001; **338**: 3–34.
35. Wishart DS, Sykes BD. The ¹³C chemical-shift index: A simple method for the identification of protein secondary structure using ¹³C chemical-shift data. *J. Biomol. NMR* 1994; **4**: 171–180.
36. Schweimer K, Hoffmann S, Bauer F, Friedrich U, Kardinal C, Feller SM, Biesinger B, Sticht H. Structural investigation of the binding of a herpesviral protein to the SH3 domain of tyrosine kinase Lck. *Biochemistry* 2002; **41**: 5120–5130.
37. Wishart DS, Bigam CG, Holm A, Hodges RS, Sykes BD. ¹H, ¹³C and ¹⁵N random coil NMR chemical shifts of the common amino acids. I. Investigations of nearest-neighbor effects. *J. Biomol. NMR* 1995; **5**: 67–81.
38. Hol WG. The role of the alpha-helix dipole in protein function and structure. *Prog. Biophys. Mol. Biol.* 1985; **45**: 149–195.
39. Huyghues-Despointes BM, Scholtz JM, Baldwin RL. Effect of a single aspartate on helix stability at different positions in a neutral alanine-based peptide. *Protein Sci.* 1993; **2**: 1604–1611.
40. Almeida FC, Opella SJ. fd coat protein structure in membrane environments: structural dynamics of the loop between the hydrophobic trans-membrane helix and the amphipathic in-plane helix. *J. Mol. Biol.* 1997; **270**: 481–495.
41. Kay LE, Torchia DA, Bax A. Backbone dynamics of proteins as studied by ¹⁵N inverse detected heteronuclear NMR spectroscopy: application to staphylococcal nuclease. *Biochemistry* 1989; **28**: 8972–8979.
42. Yao J, Chung J, Eliezer D, Wright PE, Dyson HJ. NMR structural and dynamic characterization of the acid-unfolded state of apomyoglobin provides insights into the early events in protein folding. *Biochemistry* 2001; **40**: 3561–3571.